DOI: 10.1002/anie.201000270

Nanostructures

Noble-Metal-Promoted Three-Dimensional Macroassembly of Single-Layered Graphene Oxide**

*Zhihong Tang, Shuling Shen, Jing Zhuang, and Xun Wang**

The integration of nanostructured materials into macroscopic devices that can translate phenomena at the nanoscale to the macroscopic level has proved key to paving the way to realizing applications of nanomaterials.[1] To date, although remarkable progress has been made in the self-assembly of building blocks such as nanocrystals, nanotubes, nanowires, and the newly discovered graphenes,[2–10] very little success has been achieved with three-dimensional (3D) macroscale assemblies. Herein we report the controlled assembly of single-layered graphene oxide (GO) into 3D macrostructures promoted by a noble-metal nanocrystal (Au, Ag, Pd, Ir, Rh, or Pt, etc.). Although the density of such macroassemblies is very low (ca. 0.03 $\mathrm{g\,cm^{-3}}$), they have shown excellent mechanical properties, and have been utilized as fixed-bed catalysts for a Heck reaction resulting in both 100 % selectivity and conversion. We expect our endeavor may further the research and practical applications of graphene-based materials.

Graphene is a well-defined two-dimensional structure of carbon atoms. It has received a great deal of attention because of its unique electronic, thermal, and mechanical properties.[11–13] Micromechanical cleavage from highly ordered pyrolytic graphite (HOPG) and the reduction of exfoliated graphite oxide sheets (graphene oxide, GO) are commonly used to produce graphene;[14–28] the reduction of GO appears to be a viable approach to the large-scale production of graphene. GO is usually prepared by oxidation of graphite powder with strong oxidants such as a mixture of concentrated sulfuric acid and potassium permanganate. The abundant oxygen-containing groups on GO endow it with excellent aqueous dispersion and make it easy to modify.[16–25] Recently, efforts have focused on the fabrication of graphene films through the self-assembly of the well-dispersed GO or functionalized graphene sheets.[20–23] Herein, we demonstrate that the 3D assembly of GO into macroscopic porous structures has been achieved successfully with the assistance of noble-metal nanocrystals (Au, Ag, Pd, Ir, Rh, Pt, etc.). The macroscopic size of the obtained samples can be easily controlled by adjusting the volume of the vessel, and the microstructure (the number of the pores and the pore diameter) can be controlled by varying the effective concentration of GO. These results mean that the macroscopic and microscopic structure of the sample can be controlled in one step. It not only provides a simple way to fabricate porous structures from GO, but also shows that the GO can self-assemble into more complicated 3D structures. Furthermore, the combination of noble-metal nanocrystals and the GO single layers may result in some interesting properties. As an example, we show that the Pd-embedded assemblies exhibited excellent catalytic activity and selectivity for the Heck reaction; this indicates that the self-assembled 3D structure is an ideal catalyst for a fixed- or fluid-bed reactor.

An important property of GO is that it can be readily exfoliated and forms stable colloidal suspensions in water. In our work, a dilute (1 $\mathrm{mg\,mL^{-1}}$) suspension of GO is prepared by using ultrasound methods, and the suspension then undergoes mild centrifugation. The as-prepared colloidal suspensions mainly comprise GO sheets with uniform thickness. Figure 1 a shows the atomic force microscopy (AFM) image of a typical GO sheet, and Figure 1 b shows the corresponding height profile. It shows that the graphene monolayer is irregular, having a height of about 0.7 nm and an edge that is slightly higher because of the crinkles; this data is consistent with the height of a GO monolayer.[21,22,26] There are hardly any GO sheets that are either thicker or thinner than 0.7 nm, indicating the complete exfoliation of GO in the experiment.

When the GO suspension containing a noble-metal salt and glucose is hydrothermally treated at high temperature, a 3D structure is obtained. To obtain an unchanged sample, a freeze-drying process is needed. Figure 1 c–e shows macroscopic views of the 3D self-assembled samples. The cylindrical morphology of the sample conforms to the morphology of the vessel. It is interesting that the size of the obtained samples can be controlled easily by the volume of the container. When 35 mL of the GO mixture is contained in a vessel having a volume of 50 mL, the diameter of the obtained cylinder is about 1.2 cm and the height is about 2 cm (Figure 1 c,d); when 20 mL of GO mixture is placed in a 30 mL vessel, the diameter and height of the sample decrease to about 0.7 cm and 1.2 cm, respectively (Figure 1 e). Furthermore, when the effective concentration of the GO suspension is changed, the size of the 3D self-assembled sample is not changed as long as the volume of the GO mixture is maintained. This result indicates that the size of the sample is mainly determined by the volume of the container, and the larger sample can be easily prepared provided the container is large enough. Interestingly, the 3D cylinder exhibits considerable mechanical strength. (Figure 1 f–h). Figure 1 g visually shows that the 3D cylinder can support a weight of at least 330 g even though

---

[*] Dr. Z. H. Tang, Dr. S. L. Shen, Prof. J. Zhuang, Prof. X. Wang
Department of Chemistry, Tsinghua University
Beijing 100084 (P. R. China)
Fax: (+86) 10-6279-2791
E-mail: wangxun@mail.tsinghua.edu.cn

[**] This work was supported by the NSFC (20725102, 20971078, 20921001), the Fok Ying Tung Education Foundation (111012), and the State Key Project of Fundamental Research for Nanoscience and Nanotechnology (2006CB932301).

Supporting information for this article is available on the WWW under http://dx.doi.org/10.1002/anie.201000270.

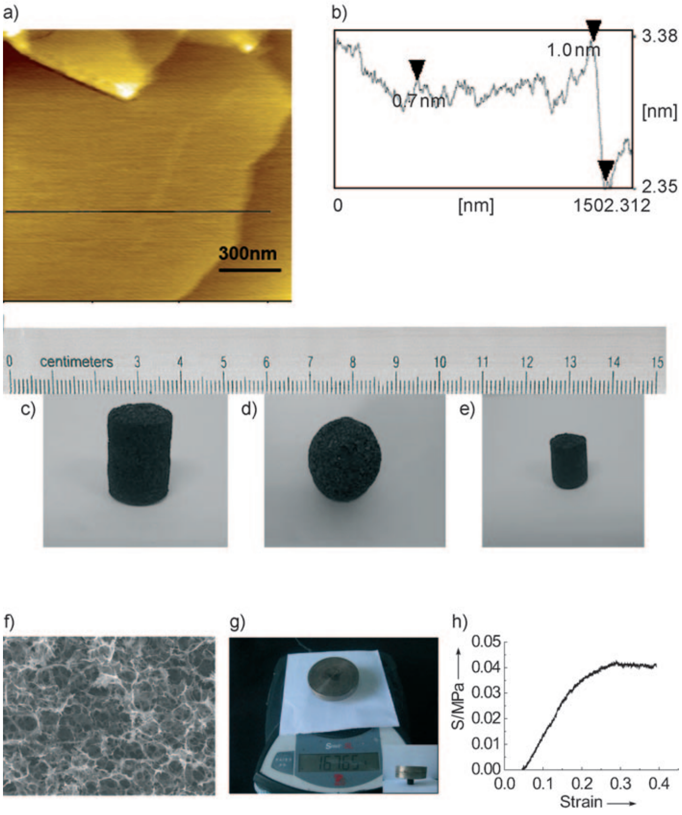

Figure 1. a) AFM image of a graphene oxide monolayer; the line indicates the direction of the height profile in (b). c–e) Photographic images of the freeze-dried 3D structures prepared by the self-assembly of graphene oxide with the assistance of a noble metal; c) the front view and d) bottom view of the sample prepared when 35 mL of graphene oxide was used. e) The front view of the sample prepared when 20 mL of graphene oxide was used. f) The SEM image of the sample in (c). g) Photo showing an iron plate weighing 167 g placed on the 3D cylinder; the inset shows that the sample can endure two iron plates. h) The strain–stress curve of the sample as determined from a compressive test. S = stress.

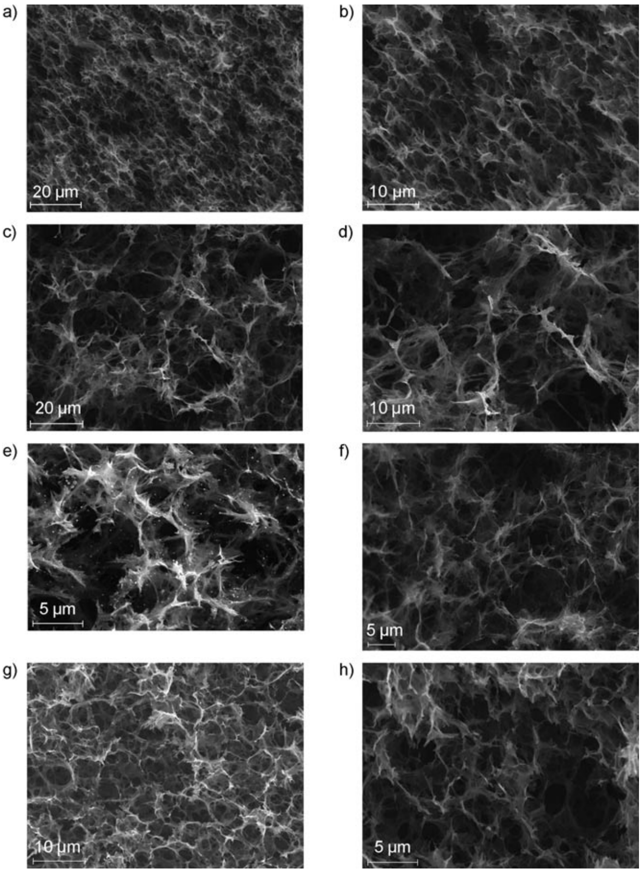

Figure 2. a,b) SEM images of the sample prepared when the concentration of the graphene oxide suspension was 0.1 mg mL^{-1}. c,d) SEM images of the sample obtained when the concentration of the graphene oxide suspension was 0.07 mg mL^{-1}. SEM images of the 3D structure containing Au (e), Pt (f), Ir (g), and Ru (h).

the cylinder itself weighs only 80 mg (estimated density of ca. 30 mg cm^{-3}). The exact mechanical properties of the sample were additionally tested by a universal testing machine. The strain–stress curve of the sample and the compressive strength that the sample supports as it varies with time are shown in Figure 1h and Figure S1 (see the Supporting Information), respectively. The compressive strength and compress modulus are approximately 0.042 MPa and 0.26 MPa, respectively, as calculated from the figures. The sample is also conductive as a result of the reduction of GO and the high conductivity of graphene; the average conductivity is about 2.5×10^{-3} S cm^{-1} as obtained by testing 10 samples.

Detailed information of the prepared samples was obtained from scanning electron microscopy (SEM), transmission electron microscopy (TEM), and AFM images. The SEM images (Figure 2a–d) clearly show that the porous structure is formed in the presence of Pd; the same porous structure can also be formed when other noble metals, such as Au, Ir, Pt, etc., are used instead of Pd (Figure 2e–h). The SEM images (Figure 2a,b) indicate that the pores are uniformly arranged and the pore diameter is about 2 µm when the GO suspension is 1 mg mL^{-1}. However, the pore diameter increases dramatically (up to 6 µm) when the GO suspension is reduced to 0.6 mg mL^{-1} (Figure 2c,d), indicating that the pore structure of the samples can be easily tuned by adjusting the effective concentration of the GO suspension.

The noble-metal/GO heterostructure of the self-assembled sample is illustrated by the morphological analyses. Figure 3a shows an AFM image of a typical GO monolayer bearing nanoparticles, and Figure 3b shows the corresponding height profile of the sheet. The height of the sheet is about 1 nm, indicating the GO monolayer contained within the 3D self-assembled structure. Compared with the initial state of the GO, the carbon sheet bearing nanoparticles is more corrugated,[27] and many particles scatter upon the corrugation, which might act as active sites for the self-assembly of GO. Figure 3c,d shows the TEM images of the heterostructure dispersed in water. The nanoparticles are scattered randomly upon the transparent carbon sheets without obvious aggregation, and few nanoparticles are spread out on the support, indicating that the majority of the particles combined with the support. Statistical analysis of the size of the nanoparticles, obtained from counting approximately 100 nanoparticles from different carbon sheets, indicates that more than 60 % of the particles have a size that is less than

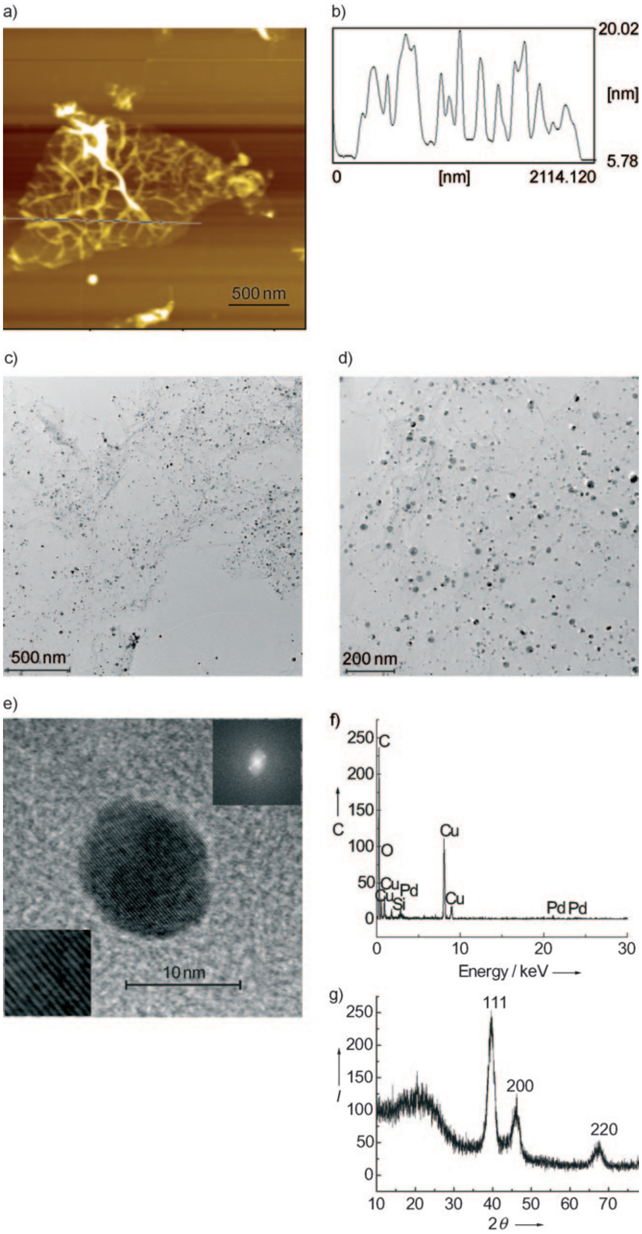

Figure 3. a) AFM image of a graphene oxide monolayer bearing Pd nanoparticles; the line indicates the direction of the height profile in (b). c–e) TEM images of graphene oxide bearing Pd nanoparticles. f) EDX analysis of the sample in (e). g) XRD pattern of the Pd-containing sample. C = counts *I* = intensity.

10 nm. The lattice spacing in the HRTEM image (Figure 3e, inset) calculated by the fast Fourier transform (FFT) pattern is about 0.2250 nm, which is consistent with the distance of (111) lattice spacing of the Pd crystal, and the energy disperse X-ray (EDX) analysis (Figure 3 f) also reveals the presence of Pd nanoparticles. The XRD pattern of the cylinder (Figure 3g) additionally indicates the formation of Pd nanoparticles. However, no obvious peaks for graphite or graphite oxide are observed in the XRD pattern, indicating that the regular stacks of the graphite or graphite oxide have been destroyed.

To investigate the mechanism of formation of these 3D assemblies, control experiments were carried out by hydrothermal treatment of glucose and GO without noble metals. When the same amount of glucose and GO were used, a 3D assembly of GO was not obtained and the final products were usually powders, indicating that the noble metal plays key role in the assembly process of single-layer GO. When the amount of glucose was increased to 3–4 g (the amount of GO remained unchanged), the macroscopic structure of a cylinder was also obtained; however, the microstructure of the assembly was quite different from that of noble metal bearing assembly. There were many thick layers in the 3D self-assembled samples (see Figure S2 a,b in the Supporting Information), and the randomly packed, thick layers formed a loose structure. From the magnified images (see Figure S2 c,d in the Supporting Information), it can be seen clearly that the thick layers comprise many closely packed thin layers. This phenomenon indicates that the metal particles play an important role in the formation of the porous structure (see Figure S2 in the Supporting Information).

The role of the metal particles in the formation of the 3D self-assembled porous structure was additionally confirmed by dissolving Pd nanoparticles in aqua regia. When the nanoparticles were removed, the regular shape of the cylinder was destroyed (see Figure S3 a in the Supporting Information), and only the collapsed, fragile, irregular structure remained. However, when the 3D structure without a noble metal (obtained by using 3–4 g glucose) was treated by aqua regia under the same conditions, the 3D structure remained integrated (see Figure S3 b in the Supporting Information), which indicates that the structure of graphene is not destroyed by aqua regia at room temperature, and the main function of aqua regia is to remove the Pd nanoparticles. The SEM images of the Pd-containing sample that was treated with aqua regia (see Figure S3 c in the Supporting Information) demonstrate that the pore diameter is larger than 10 μm, which is much larger than that in Figure 2 b. This difference indicates that many walls collapse after removal of the Pd nanoparticles, and it can therefore be concluded that the Pd nanoparticles are an important part of the framework of the 3D cylinder.

Glucose is also necessary in the formation of 3D cylinder, as it not only reduces the noble-metal salt, but also increases the mechanical strength of the self-assembled structure. Figure S4 (see the Supporting Information) illustrates the mass spectrometry (MS) data for the remaining solution after hydrothermal treatment. It shows that polymers, formed during the hydrothermal treatment in the presence of GO and a noble-metal salt, have a low degree of polymerization (the molecular weight is less than 1000). Some polymers may fill in the 3D cylinder and some may react with the functional groups on the GO, and therefore enhance the mechanical strength of the cylinder to some extent. Of course, some polymers may dissolve in the water, and these are detected by MS methods.

As mentioned above, when the sample is prepared without the noble-metal salt, thick layers composed of many closely packed thin layers are formed. The exfoliated GO must rearrange to form stable structures under the vapor pressure. It is reported that the preferential rearrangement of the exfoliated GO is face-to-face.[21] Thus, the closely packed layer is formed, as demonstrated in Figure 4a. This is not the case when the Pd nanoparticles are present in the system. The Pd nanoparticles anchored onto the GO sheet could act as active sites for assembly with another GO sheet. Since there are many corrugations formed in the Pd-bearing GO, the assembly of GO sheets by particles would form porous structures (Figure 4b).

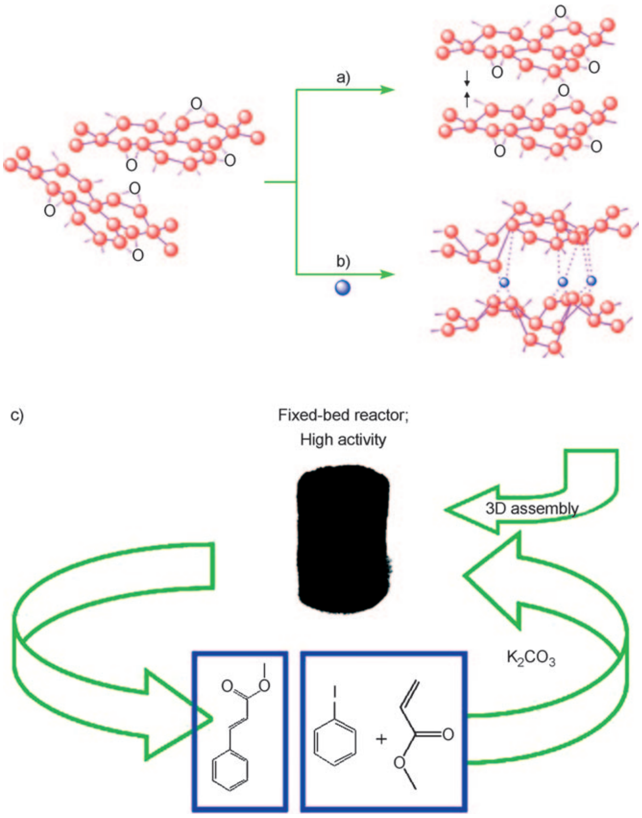

Figure 4. Schematic representation of the assembly of a) the graphene oxide sheets and b) the graphene oxide sheets with a noble metal (e.g., Pd). c) Schematic of a Heck reaction in a fixed-bed reactor.

Pd is a very useful catalyst for organic reactions, and GO bearing Pd nanoparticles has been successfully applied to a Suzuki reaction.[28] It is therefore possible that the Pd dispersed over the GO 3D macroassemblies would exhibit high reactivity for other Pd-catalyzed reactions. Herein we selected the Heck reaction as a model reaction for evaluating the catalytic properties of the self-assembled samples. Triethylamine was chosen as the base in the reaction in which iodobenzene and methyl acrylate were reacted in the presence of the 3D cylinder (0.1 mol% Pd) as the catalyst; the selectivity was about 92% and the conversion was 100%. Although the selectivity was rather high compared with the reported results,[29] the by-product was present. Furthermore, we found that using K_2CO_3 as base can avoid the formation of the by-product; therefore both the selectivity and conversion were 100% (below the detection limit of GC–MS), which is much higher than the results obtained when the Pd catalyst is loaded onto the other supports.[29] For organic reactions selectivity is a very important parameter for evaluating the feasibility of the reaction, and it is very hard to realize a selectivity of 100%; therefore the Pd anchored to the GO could serve as a potential catalyst in future applications. Furthermore, the high strength endurance makes it suitable for fixed-bed process in industry (Figure 4c).

In summary, we have demonstrated that the 3D self-assembly of GO, having very low density and tunable macro- and microstructures, can be achieved successfully by using a hydrothermal method. The size and microstructure of the sample can be controlled by the volume of vessel and the effective concentration of GO suspension, respectively. The obtained 3D structures exhibit high conductivity and strength endurance despite the porous structure. These assemblies have shown high catalytic activity and selectivity in the Heck reaction, and the excellent mechanical properties make this a promising catalyst for either a fixed- or fluid-bed processes in large-scale production.

Experimental Section

GO synthesis: GO was prepared from natural graphite powders according to a modified Hummers method.[21] H_2SO_4 (230 mL) was placed in a flask, which was then cooled using an ice bath. $NaNO_3$ (5 g) and graphite (10 g) were then added to the H_2SO_4 and stirred vigorously. Next, $KMnO_4$ (30 g) was slowly added to the reaction flask, and the reaction temperature was then maintained below 20 °C in an ice bath. The flask containing the reaction mixture was then transferred to a water bath at a temperature of 35 °C, and the reaction mixture was stirred for about 30 min until a thick paste had formed. Water (460 mL) was then added and the reaction temperature increased to 98 °C, at which point the reaction mixture was stirred for about 40 min. Finally, the mixture was diluted to 1400 mL, followed by the slow addition of 3 mL of 30% aq. H_2O_2. A yellow dispersion was obtained and washed repeatedly with water to remove the remaining salt, and the solid was then dried under vacuum (60 °C) for about 3 days.

Self-assembly of GO: The self-assembly of GO involves a noble-metal salt such as $PdCl_2$, $HAuCl_4$, $RhCl_3$, etc, and glucose. All the chemicals were used as received without additional purification. In a typical reaction, a 1 $mg\,mL^{-1}$ suspension of GO was prepared by the sonication of GO (0.6 g) in water (500 mL) for about 1.5 h, after which the thick layers were removed by mild centrifugation (3 krpm for 10 min). The GO suspension (35 mL), glucose (1.75 g), and $PdCl_2$ (10 mg) were combined and stirred for about 30 min. The mixture was then transferred into a Teflon-lined stainless-steel autoclave, and treated hydrothermally at 120 °C for 20 h. After the hydrothermal treatment was completed, the autoclave was cooled and the as-obtained sample was washed with distilled water and then freeze-dried for characterization.

The general procedure for the Heck reaction and details on the characterization of the self-assembled samples are given in the Supporting Information.

Received: January 16, 2010
Revised: March 26, 2010

Keywords: graphene · nanostructures · noble metals · self-assembly

[1] J. M. Phillips, *MRS Bull.* **2006**, *31*, 44 – 49.
[2] G. M. Whitesides, B. Grzybowski, *Science* **2002**, *295*, 2418 – 2421.
[3] Y. Lin, A. Boker, J. He, K. Sill, H. Xiang, C. Abetz, X. Li, J. Wang, T. Emrick, S. Long, Q. Wang, A. Balazs, T. P. Russell, *Nature* **2005**, *434*, 55 – 59.
[4] E. V. Shevchenko, D. V. Talapin, N. A. Kotov, S. O'Brien, C. B. Murray, *Nature* **2006**, *439*, 55 – 59.
[5] Z. Tang, N. A. Kotov, M. Giersig, *Science* **2002**, *297*, 237 – 240.
[6] H. W. Zhu, C. L. Xu, D. H. Wu, B. Q. Wei, R. Vajtai, P. M. Ajayan, *Science* **2002**, *296*, 884 – 886.
[7] Y. Huang, X. Duan, Q. Wei, C. M. Lieber, *Science* **2001**, *291*, 630 – 633.
[8] K. Jiang, Q. Li, S. Fan, *Nature* **2002**, *419*, 801.
[9] L. Xiao, Z. Chen, C. Feng, L. Liu, Z. Bai, Y. Wang, L. Qian, Y. Zhang, Q. Li, K. Jiang, S. Fan, *Nano Lett.* **2008**, *8*, 4539 – 4545.
[10] Y. Huang, X. Duan, Y. Cui, L. J. Lauhon, K. Kim, C. M. Liber, *Science* **2001**, *294*, 1313 – 1317.
[11] K. S. Novoselov, A. K. Geim, S. V. Morozov, D. Jiang, Y. Zhang, S. V. Dubonos, L. V. Grigorieva, A. A. Firsov, *Science* **2004**, *306*, 666 – 669.
[12] K. S. Novoselov, A. K. Geim, S. V. Morozov, D. Jiang, M. I. Katsnelson, I. V. Grigorieva, S. V. Dubons, A. A. Firsov, *Nature* **2005**, *438*, 197 – 200.
[13] C. N. R. Rao, A. K. Sood, K. S. Subrahmanyam, A. Govindaraj, *Angew. Chem.* **2009**, *121*, 7890 – 7916; *Angew. Chem. Int. Ed.* **2009**, *48*, 7752 – 7777.
[14] K. A. Worsley, P. Ramesh, S. K. Mandal, S. Niyogi, M. E. Itkis, R. C. Haddon, *Chem. Phys. Lett.* **2007**, *445*, 51 – 56.
[15] X. L. Li, X. R. Wang, L. Zhang, S. Lee, H. Dai, *Science* **2008**, *319*, 1229 – 1232.
[16] G. Wang, J. Yang, J. Park, X. Gou, B. Wang, H. Liu, J. Yao, *J. Phys. Chem. C* **2008**, *112*, 8192 – 8195.
[17] C. Chen, Q. Yang, Y. Yang, W. v. Y. Wen, P. Hou, M. Wang, H. Cheng, *Adv. Mater.* **2009**, *21*, 3007 – 3011.
[18] A. V. Talyzin, V. L. Solozhenko, O. O. Kurakevych, T. Szabo, I. Dekany, A. Kurnosov, V. Dmitriev, *Angew. Chem.* **2008**, *120*, 8392 – 8395; *Angew. Chem. Int. Ed.* **2008**, *47*, 8268 – 8271; *Angew. Chem.* **2008**, *120*, 8392 – 8395.
[19] S. Stankovich, D. A. Dikin, R. D. Piner, K. A. Kohlhaas, A. Kleinhammes, Y. Jia, Y. Wu, S. T. Nguyen, R. S. Ruoff, *Carbon* **2007**, *45*, 1558 – 1565.
[20] Y. Xu, H. Bai, G. Lu, C. Li, G. Shi, *J. Am. Chem. Soc.* **2008**, *130*, 5856 – 5857.
[21] L. J. Cote, F. Kim, J. Huang, *J. Am. Chem. Soc.* **2009**, *131*, 1043 – 1049.
[22] J. Shen, Y. Hu, C. Li, C. Qin, M. Shi, M. Ye, *Langmuir* **2009**, *25*, 6122 – 6128.
[23] D. A. Dikin, S. Stankovich, E. J. Zimney, R. D. Piner, G. H. B. Dommett, G. Evmenenko, S. T. Nguyen, R. S. Ruoff, *Nature* **2007**, *448*, 457 – 460.
[24] Z. Wei, D. E. Barlow, P. E. Sheehan, *Nano Lett.* **2008**, *8*, 3141 – 3145.
[25] Y. Xu, Z. Liu, X. Zhang, Y. Wang, J. Tian, Y. Huang, Y. Ma, X. Zhang, Y. Chen, *Adv. Mater.* **2009**, *21*, 1275 – 1279.
[26] J. I. Paredes, S. V. Rodil, A. M. Alonso, J. M. D. Tascon, *Langmuir* **2008**, *24*, 10560 – 10564.
[27] C. Xu, X. Wang, J. Zhu, *J. Phys. Chem. C* **2008**, *112*, 19841 – 19845.
[28] G. M. Scheuermann, L. Rumi, P. Steurer, W. Bannwarth, R. Mulhaupt, *J. Am. Chem. Soc.* **2009**, *131*, 8262 – 8270.
[29] X. Fan, M. G. Manchon, K. Wilson, S. Tennison, A. Kozynchenko, A. A. Lapkin, P. K. Plucinski, *J. Catal.* **2009**, *267*, 114 – 120.